SUPPLEMENTARY INFORMATION

Foundation model for efficient biological discovery in single-molecule data

Jieming Li[†1]*, Leyou Zhang[†2], Alexander Johnson-Buck[3], and Nils G. Walter[3]*

[1]Bristol Myers Squibb, New Brunswick, NJ, USA

[2]Google, New York City, NY, USA

[3]Single Molecule Analysis Group, Department of Chemistry, The University of Michigan, Ann Arbor, MI, USA

[†]These authors contributed equally to this work

*jieming.li@bms.com (or jmli@umich.edu), nwalter@umich.edu

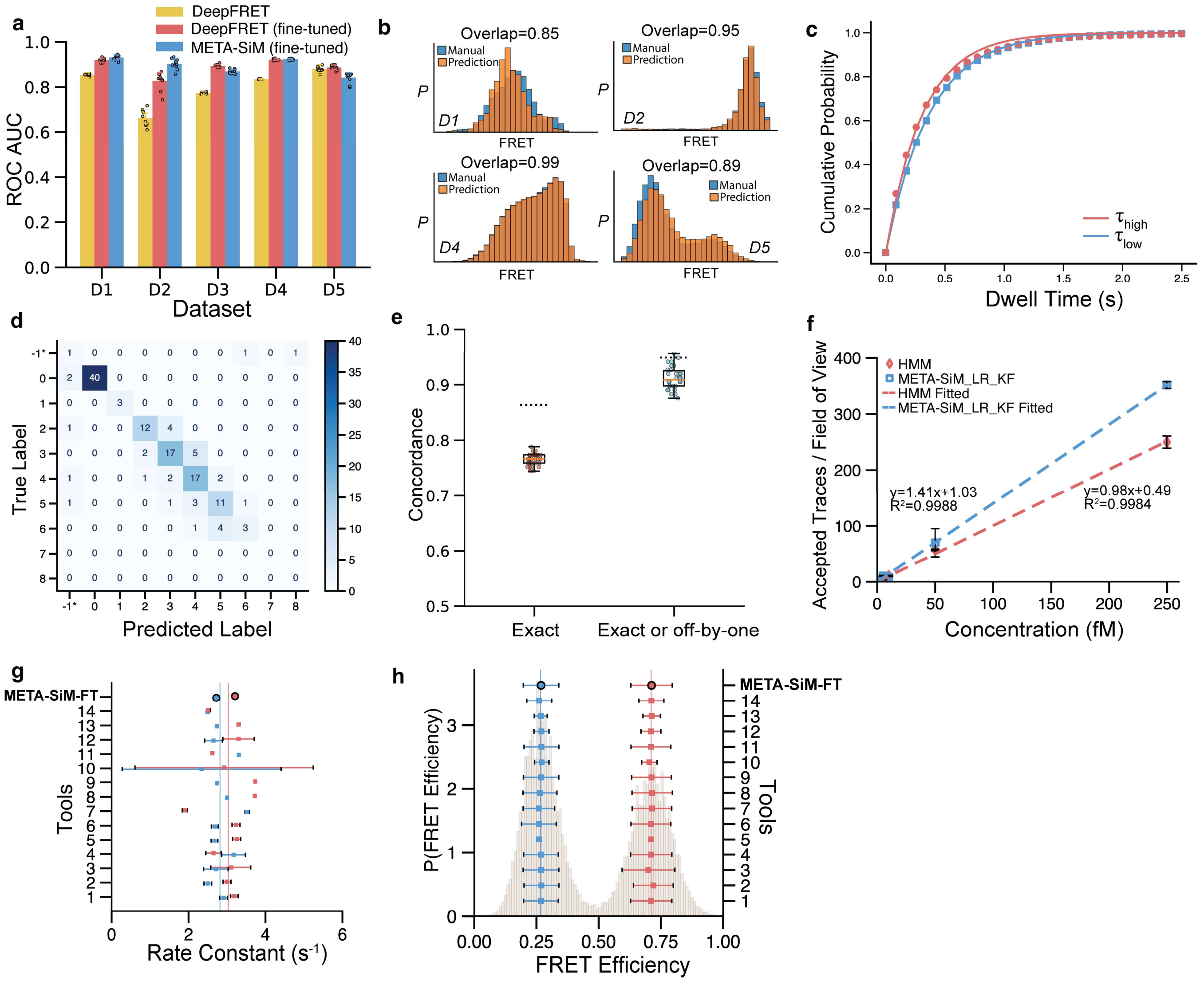

Supplementary Fig. 1| Performance of META-SiM in various downstream tasks. a, The area under the receiver-operating characteristic curve (ROC AUC) for trace classification by META-SiM and DeepFRET compared to manual analysis. **b,** Representative FRET histograms based on traces curated and segmented by META-SiM versus manual analysis. **c**, A distribution of dwell time predicted by the model is fit with single exponential distributions to yield transition rate constants. **d,** A representative confusion matrix comparing the labels from manual counting ("True Label") to the labels predicted by META-SiM. **e,** Concordance between manual counting and predictions by META-SiM that either match exactly or differ by no more than one step. **f**, Standard curve for T790M generated by META-SiM and HMM analysis. **g, h**, Evaluation of performance in trace idealization for META-SiM (Fine-Tuned), and benchmarking against 14 other common analysis tools[1], on the basis of measured rate constants (**g**) and FRET efficiencies (**h**): (1) Pomegranate; (2) Tracy(HMM); (3) FRETboard; (4) Hidden-Markury; (5) SMACKS(SS); (6) SMACKS; (7) Correlation; (8) Edge finding(CK); (9) Edge finding(k-means); (10) Step finding; (11) STaSI; (12) MASH-FRET(bootstrap); (13) MASH-FRET(prob); (14) postFRET.

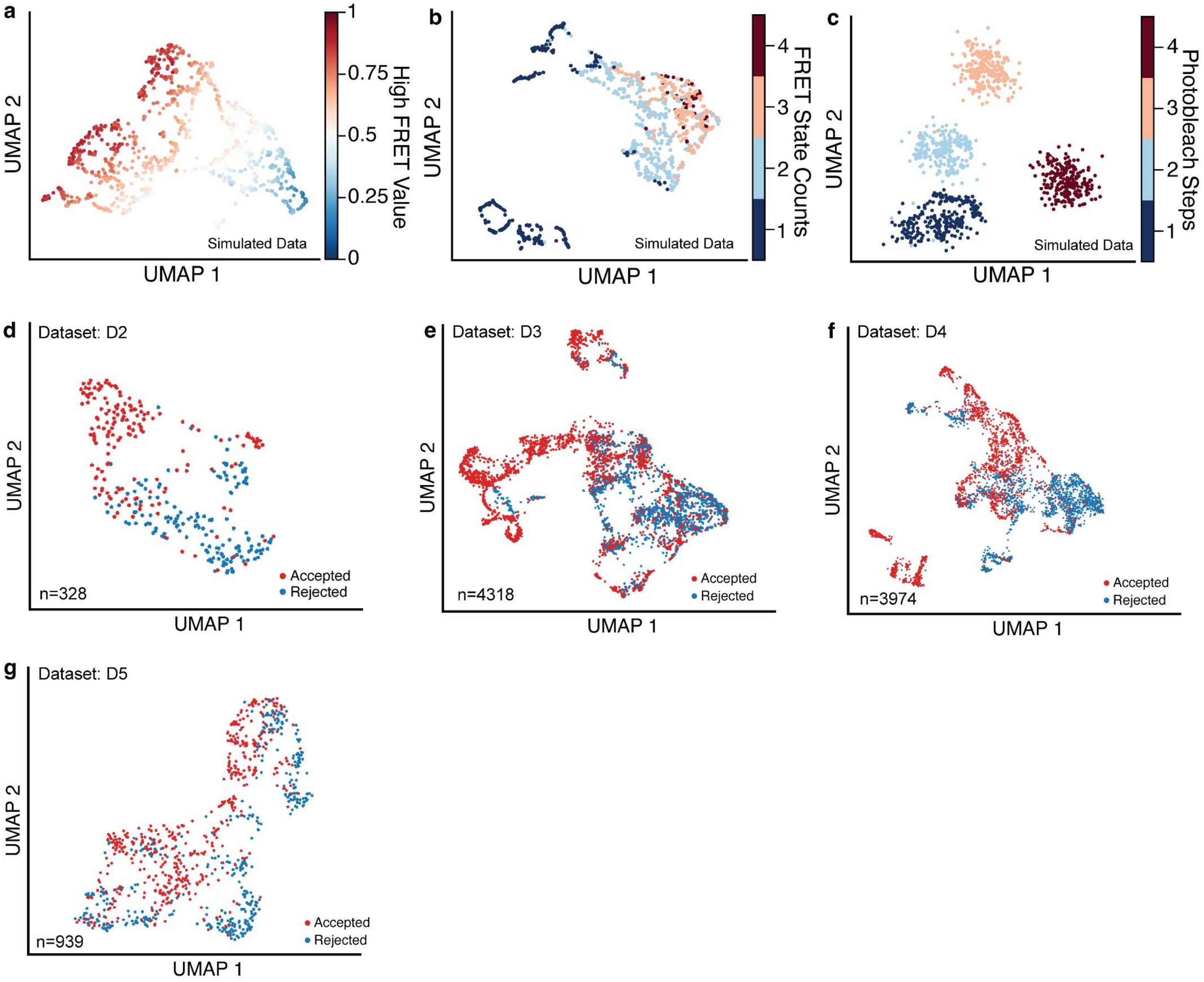

Supplementary Fig. 2 | Evaluation of UMAP projection on both simulated and experimental data. a,b,c, 2D UMAP projections of simulated traces with varying high-FRET value (**a**), number of FRET states (**b**), and number of photobleaching steps (**c**). **d,e,f,g,** 2D UMAP projection of traces from dataset D2[2], D3[3], D4[4], D5[5] that were manually accepted (red) or rejected (blue) for further analysis.

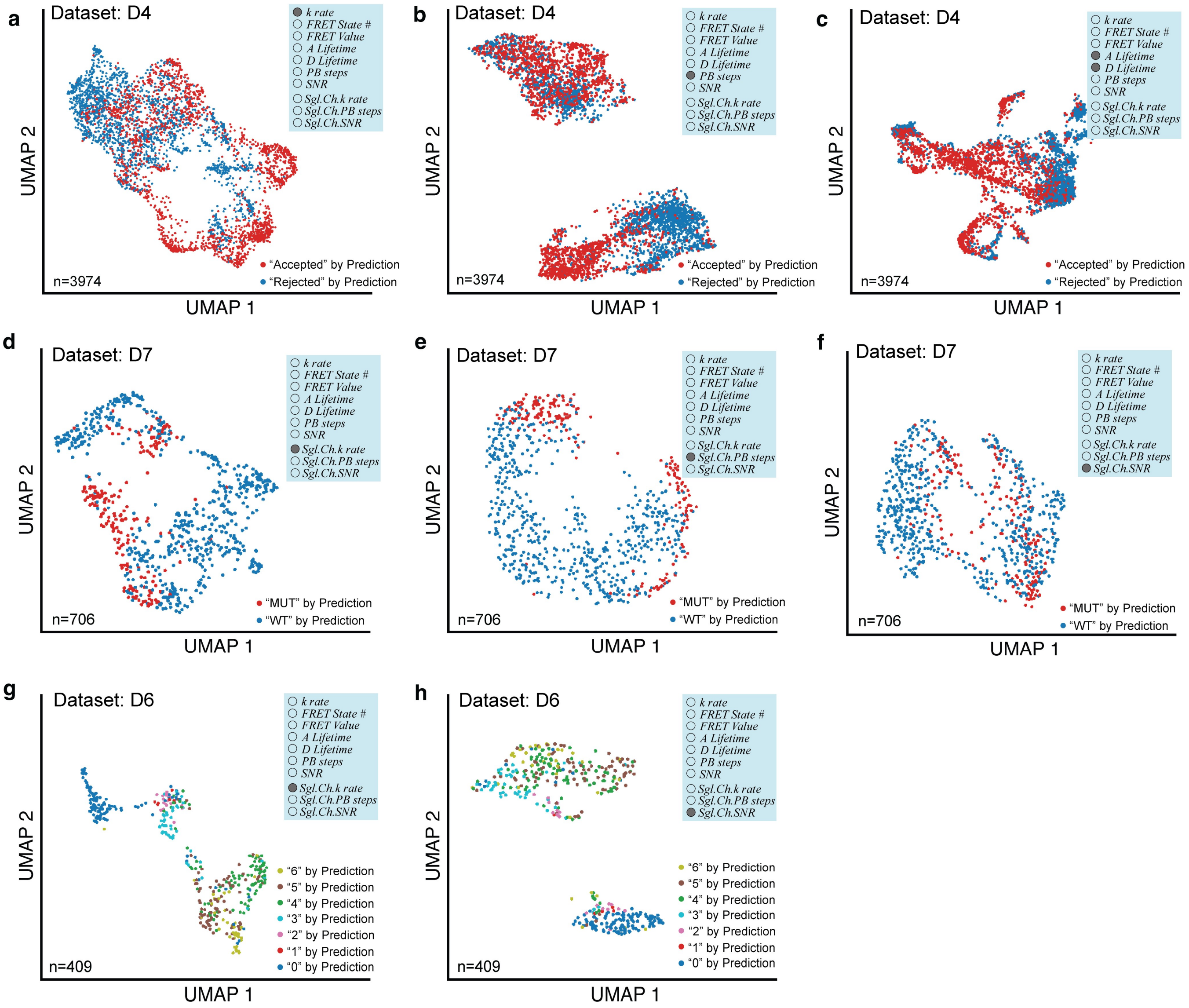

Supplementary Fig. 3 | Varying principal projections from the same dataset. a,b,c, 2D UMAP projection of dataset D4[4] based on different attributes: kinetic rate (**a**), photobleaching steps (**b**), donor and acceptor fluorophore lifetime prior to photobleaching (**c**). **d,e,f,** 2D UMAP projection of dataset D7[6] based on different attributes: single-channel kinetic rate (**d**), single-channel photobleaching steps (**e**), single-channel SNR (**f**). **g,h,** 2D UMAP projection of dataset D6 with different attributes: single-channel kinetic rate (**g**), single-channel SNR (**h**).

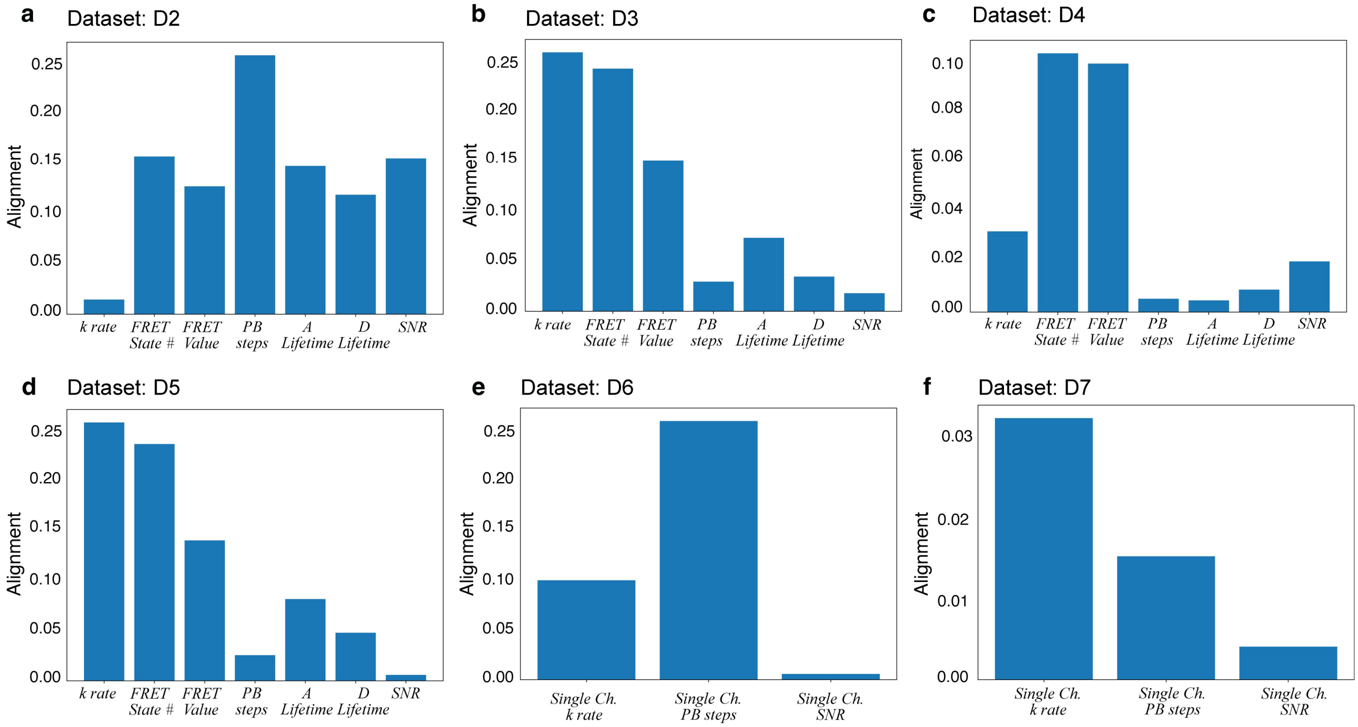

Supplementary Fig. 4 | Quantitative assessment of the alignment of individual data attributes to network predictions. a, b, c, d, e, f, Alignment of specific data analysis attributes with the META-SiM classifier fine-tuned for the different datasets D2, D3, D4, D5, D6, D7 to achieve the classification task.

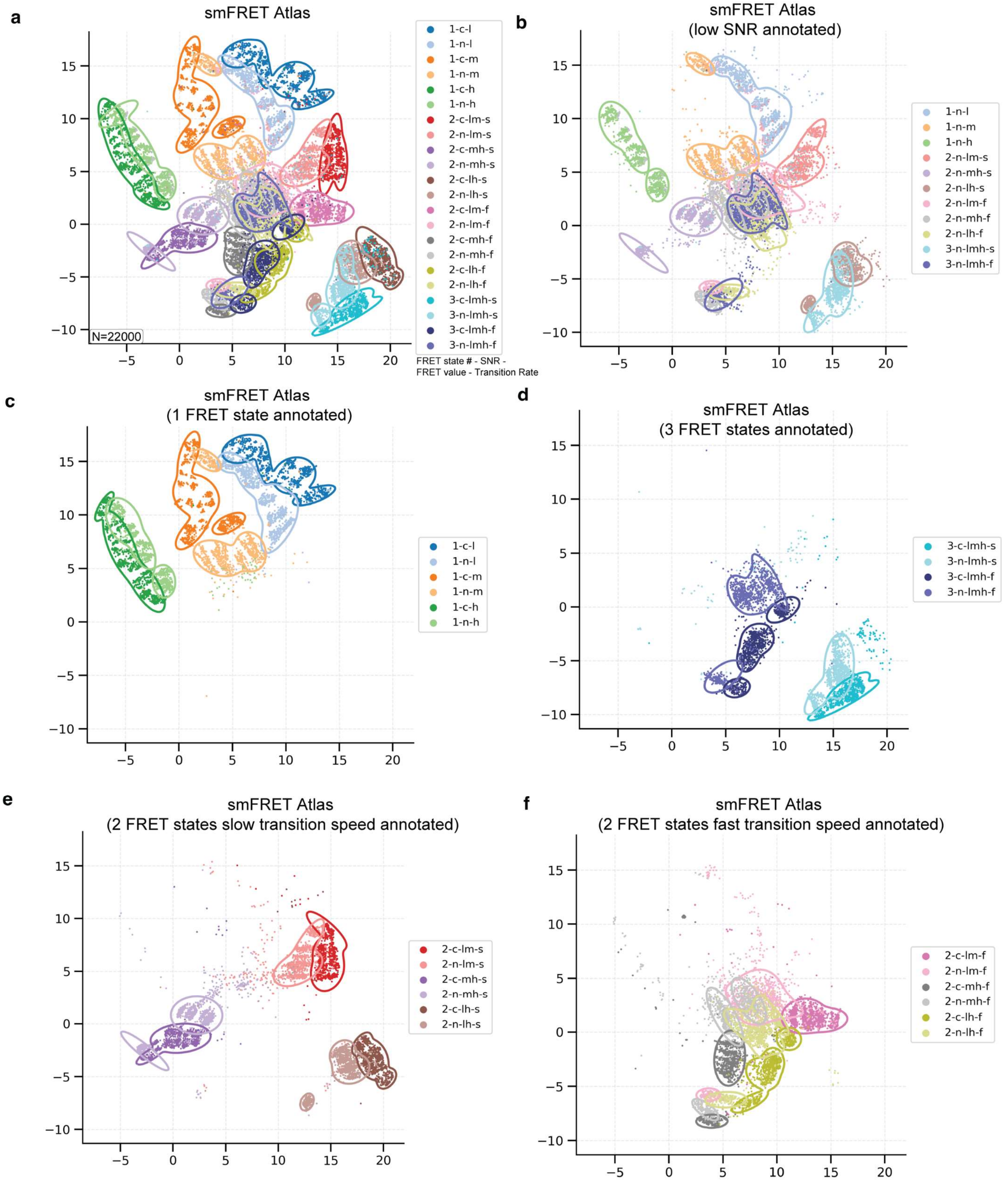

Supplementary Fig. 5 | Different annotations of the smFRET Atlas. a, An smFRET Atlas constructed with 22,000 traces derived from simulation. **b,c,d,e,f,** the same Atlas where only (**b**) low-SNR traces, (**c**) traces with a single FRET state, (**d**) traces with 3 FRET states, (**e**) traces with two FRET states and slow transitions, or (**f**) traces with two FRET states and fast transitions are plotted. Codes for cluster names (1-c-l, etc.) are listed in **Supplementary Table 3**.

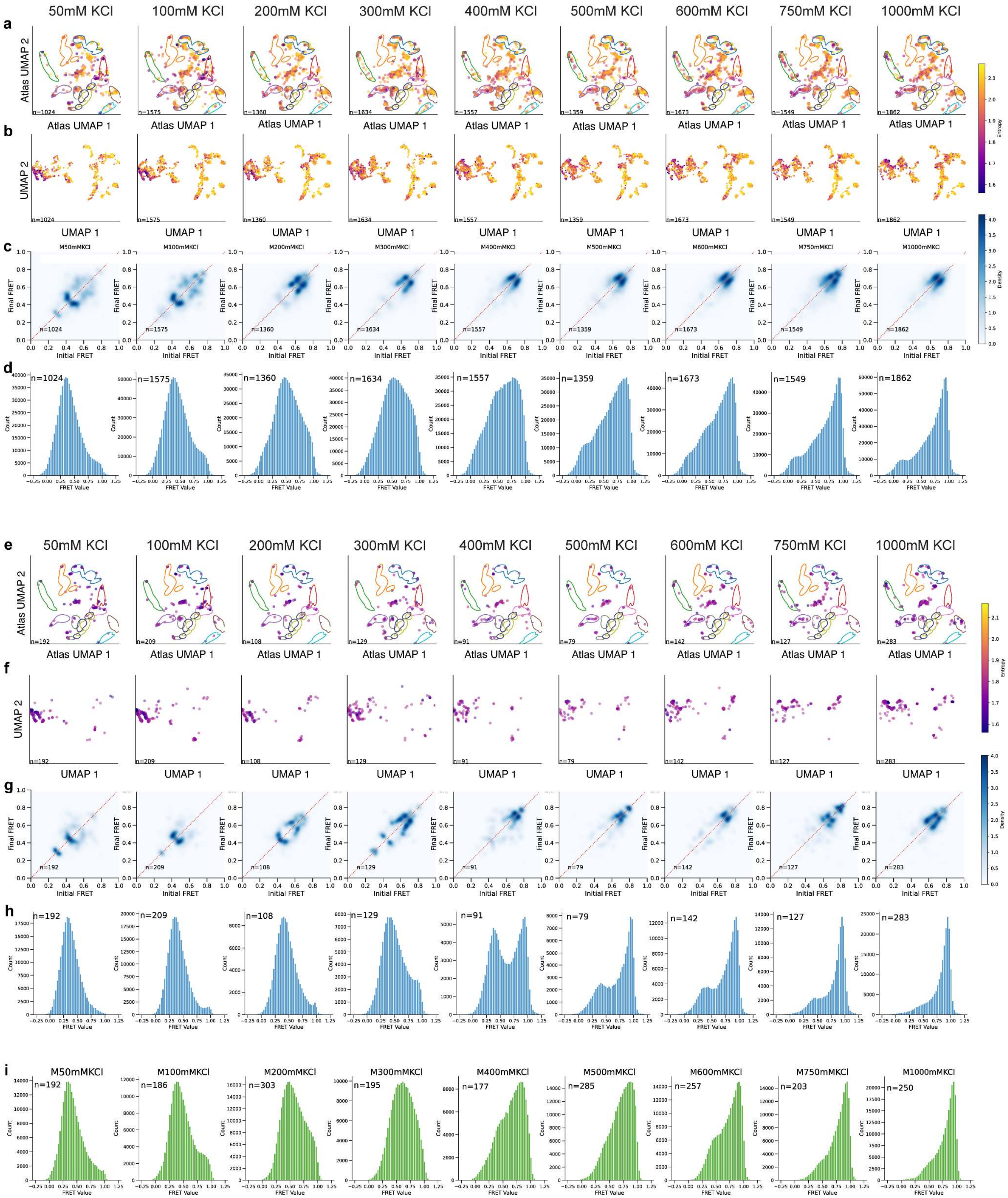

Supplementary Fig. 6 | Titration of KCl into the paused transcriptional elongation complex system (D4). a,b, 2D UMAP projections of embeddings from uncurated traces under different KCl concentrations in Atlas coordinates (**a**) and system-specific coordinates (**b**). **c,** TODPs of traces from the different KCl concentration conditions. **d,** FRET histogram of traces from the different KCl concentrations. **e,f,** 2D UMAP projections of the 10% of embeddings with lowest LSE from traces under the different KCl concentrations in Atlas coordinates (**e**) and system-specific coordinates (**f**). **g,** TODPs of 10% lowest LSE traces from the different KCl concentration conditions. **h,** FRET histograms of the 10% of traces with lowest LSE from the different KCl concentrations. **i,** FRET histograms of manually curated traces from the different KCl concentrations.

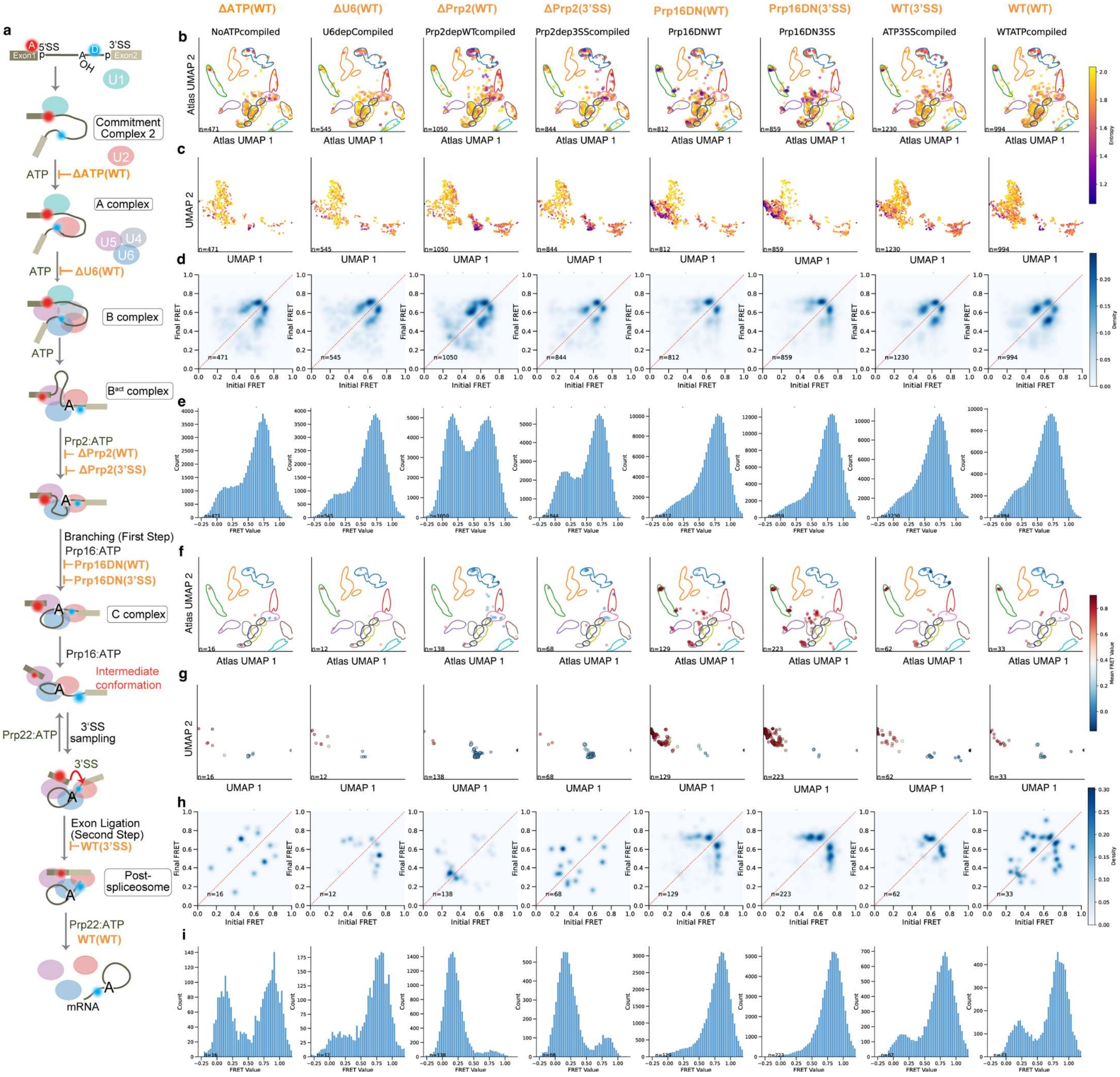

Supplementary Fig. 7 | Full smFRET characterization of the yeast pre-mRNA splicing pathway. a, Diagram of the splicing pathway. Experimental conditions used to block any further progress beyond specific steps in the pathway are annotated in orange font[7]. **b, c,** 2D UMAP projections of trace embeddings from the different experimental conditions in Atlas coordinates (**b**) and system-specific coordinates (**c**). **d,** TODPs of traces from the different experimental conditions. **e,** FRET histograms of traces from the different experimental conditions. **f, g,** 2D UMAP projections of the 10% of traces with lowest LSE under the different experimental conditions in Atlas coordinates (**f**) and system-specific coordinates (**g**). **h,** TODPs of the 10% of traces with lowest LSE from the different experimental conditions. **i,** FRET histogram of the 10% of traces with lowest LSE from the different experimental conditions.

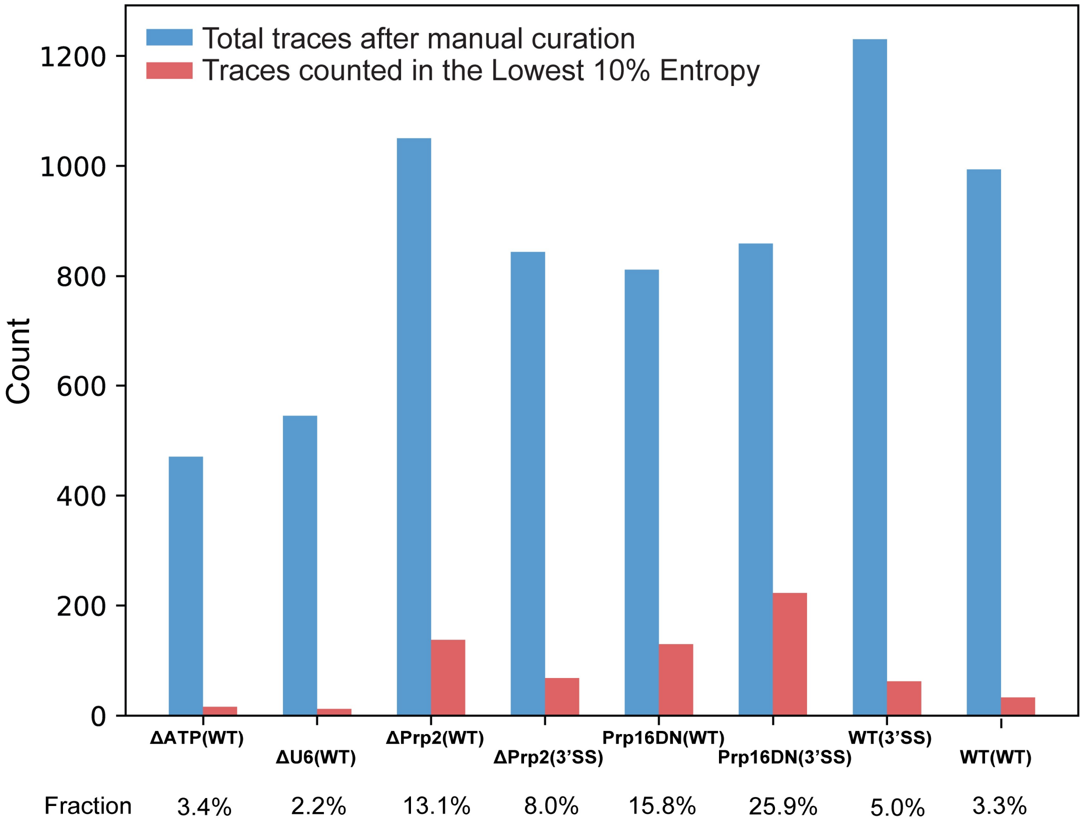

Supplementary Fig. 8 | Distribution of the 10% of traces with lowest LSE across the different experimental conditions in the splicing study. The total number count and fraction of traces from each experimental dataset that are among those with the 10% lowest LSE values is different, indicating that certain conditions exhibit a larger fraction of highly condition-specific traces.

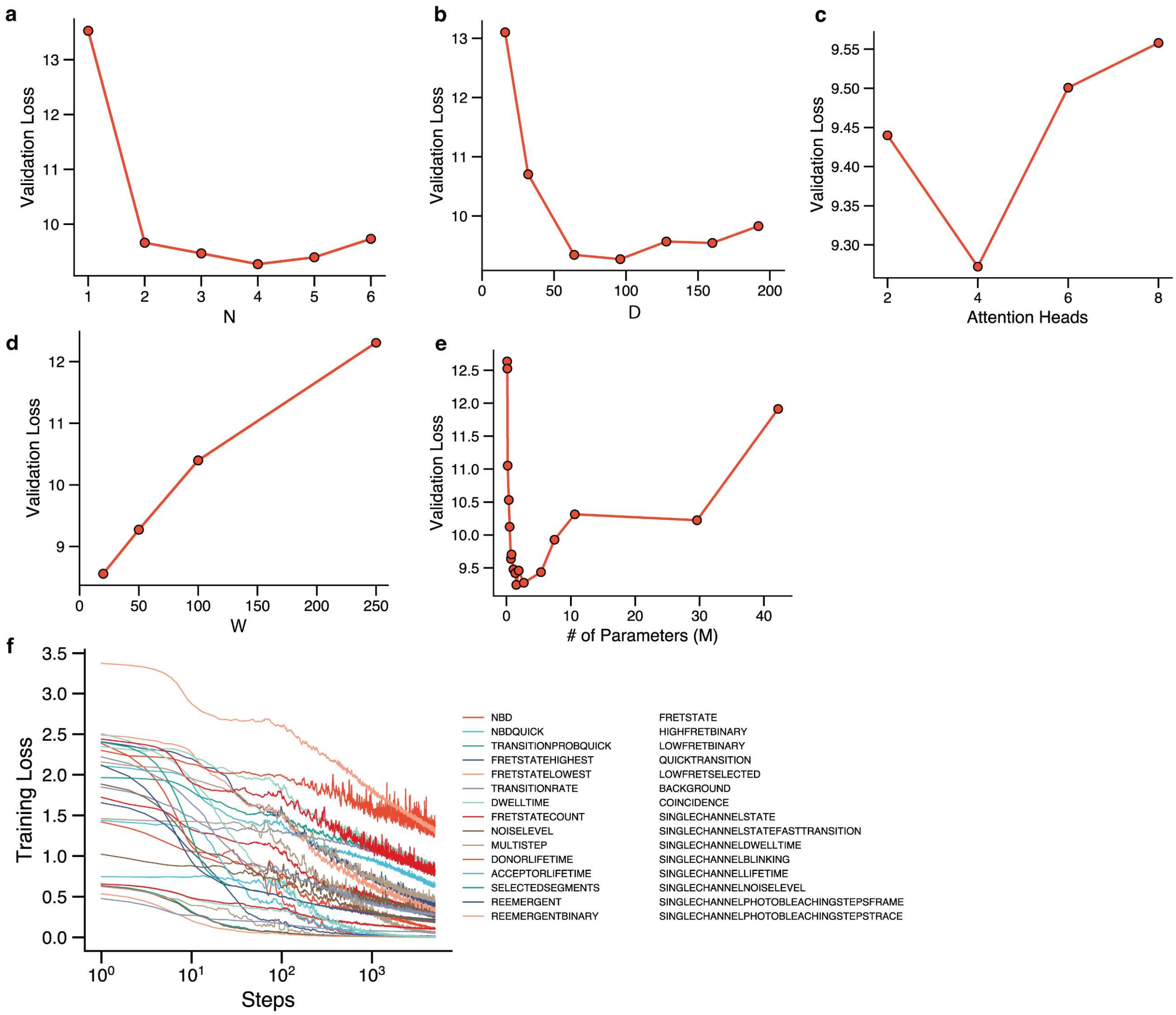

Supplementary Fig. 9 | Pre-Training results and hyperparameter evaluation. a, Impact of the number of transformer layers (N) on training effectiveness. **b,** Impact of the number of embedding vector dimensions (D) on training effectiveness. **c,** Impact of the number of Attention Heads on training effectiveness. **d,** Impact of the width of trace patches (W) used in tokenization on training effectiveness. **e,** Impact of the number of parameters (M) on training effectiveness. **f,** Loss of all training tasks as a function of pre-training steps.

Supplementary Table 1. Definition of training tasks for multi-task pre-training of META-SiM. The main data attribute for each task listed in the table was used for grouping the tasks for the principal projection and task alignment calculations in Fig. 4.

Index	Task	Definition	Main Data Attribute	Frame-level or Trace-level
1	FRET state idealization	Predict true FRET state for each time frame. Prediction is FRET value ([0, 1]) instead of FRET state index (1, 2, 3, etc.).	Kinetic rate constant	Frame-level
2	Counting the number of FRET states	Counting the number of distinct FRET states presented in a time trace.	Number of states	Trace-level
3	Identifying highest FRET state frames	Locating which frames are in the FRET state with the highest FRET value.	FRET value	Frame-level
4	Identifying lowest FRET state frames	Locating which frames are in the FRET state with lowest FRET value, and label it as true. Note that blinking and photobleached states are not considered the lowest FRET state and labeled as false.	FRET value	Frame-level
5	Identifying highest FRET state's FRET value	Identifying the highest FRET value for a time trace.	FRET value	Trace-level
6	Identifying lowest FRET state's FRET value	Identifying the lowest FRET value that is not blinking or photobleached for a time trace.	FRET value	Trace-level
7	Extracting mean dwell time	Predicting the mean dwell time of all the FRET states in a time trace.	Kinetic rate constant	Trace-level
8	Extracting signal-to-noise ratio	Predicting the signal-to-noise ratio for a time trace.	Noise	Trace-level
9	Extracting donor fluorophore lifetime	Predicting the total lifetime of the donor fluorophore for a time trace.	FRET donor lifetime	Trace-level
10	Extracting acceptor fluorophore lifetime	Predicting the total lifetime of the acceptor fluorophore for a time trace.	FRET acceptor lifetime	Trace-level
11	Counting multistep photobleaching	Counting the photobleaching steps for traces with single- or multi-step photobleaching (0-4 steps).	Photobleaching steps	Trace-level
12	Selecting segments for active FRET states	Selecting the frames of a time trace where the FRET state is either static or dynamic, but is not blinking or photobleached.	Photobleaching steps	Frame-level
13	Extracting the average kinetic rate constant	Predicting the average kinetic rate constant for a	Kinetic rate constant	Trace-level

		time trace. The ground truth is defined as the harmonic average of all kinetic rate constants that are used in the simulator for a particular trace.		
14	Identifying re-appearance of active FRET states after photobleaching	Identifying frames that are in active FRET states but occur after one or more photobleaching events. This behavior is common for experimental data where more than one fluorophore is present.	Photobleaching steps	Frame-level
15	Identifying existence of re-appearance of active FRET states after photobleaching	Identifying whether a trace has active FRET states after one or more photobleaching events. This behavior is common for experimental data.	Photobleaching steps	Trace-level
16	Counting the number of state transitions	Counting the total number of state transitions for a time trace.	Kinetic rate constant	Trace-level
17	Counting the number of state transitions for very fast dynamics	Counting the total number of state transitions for a time trace with very fast dynamics.	Kinetic rate constant	Trace-level
18	FRET state idealization for very fast dynamics	Predict true FRET state for each time frame with very fast dynamics. Prediction is FRET value ([0, 1]) instead of FRET state index (1, 2, 3, etc.)	Kinetic rate constant	Frame-level
19	Extracting average kinetic rate constant for very fast dynamics	Predicting the average kinetic rate constant for time traces with very fast dynamics.	Kinetic rate constant	Trace-level
20	Identifying if a frame is in the lowest FRET state	Identifying whether a frame in a time trace is in the FRET state with the lowest FRET value and is an active state. This task aims to help models distinguish real low FRET from photobleached states. Note that the previous prediction target of highest/lowest FRET state tasks is the FRET value, while this task's prediction target is a binary true/false label for each frame.	FRET value	Frame-level
21	Extracting background intensity	Predicting the true background intensity after the last photobleaching event for a time trace.	Noise	Trace-level

22	Identifying colocalized pairs of fluorophores	Predicting whether a time trace has more than 1 pair of fluorophores. This phenomenon is common in experimental data when two or more pairs of fluorophores overlap in space (i.e., are colocalized).	Photobleaching steps	Trace-level
23	State idealization for a single-channel time trace	Identifying true states and predict de-noised intensity for a single-channel time trace.	Single-channel kinetic rate constant	Frame-level
24	Extract the mean dwell time for a single-channel time trace	Predicting the dwell time averaged over all kinetic states in a single-channel time trace.	Single-channel kinetics rate constant	Trace-level
25	Extract the average kinetic rate constant for a single-channel time trace	Predicting the average kinetic rate constant for a time trace. The ground truth is defined as the harmonic average of all kinetic rate constants that are used in the simulator for a particular single-channel trace.	Single-channel kinetics rate constant	Trace-level
26	Identifying blinking frames for a single-channel time trace	Identifying the frames that are in a blinking state for a single-channel time trace.	Single-channel noise	Frame-level
27	Extracting fluorophore lifetime for a single-channel time trace	Predicting the total lifetime of the fluorophore before the first photobleaching event for a single-channel time trace.	Single-channel lifetime	Trace-level
28	Extracting the signal-to-noise ratio for a single-channel time trace	Predicting the signal-to-noise ratio for a single-channel time trace.	Single-channel noise	Trace-level
29	Identifying photobleaching step frames for a single-channel time trace	Locating the frames where photobleaching steps happen for a single-channel time trace.	Single-channel photobleaching steps	Frame-level
30	Counting photobleaching steps for a single-channel time trace	Counting the total number of photobleaching steps for a single-channel time trace.	Single-channel photobleaching steps	Trace

Supplementary Table 2. Description of datasets used in pre-training and downstream tasks.

Dataset Index	Tasks	Description	Data Type	Pre-Training Set Size [Trace]	Fine-tuning Set Size [Trace]	Testing Set Size [Trace]	# of Detection Channels
D1	Trace Classification & Segmentation	A toehold-exchange-based DNA walker[8]	Exp.	N/A	109	642	Two-color
D2		A DNA swinging arm[2]			82	233	
D3		A preQ$_1$ riboswitch[3]			215	4628	
D4		A paused transcriptional elongation complex[4]			137	3770	
D5		A Mn^{2+} riboswitch[5]			105	656	
D6	Stoichiometry Analysis	A photobleaching dataset from a 6-subunit protein complex bearing up to one HaloTag Alexa Fluor 660 (Alexa660) label per monomer	Exp.	N/A	261	231	One-color
D7	Kinetic Fingerprinting	A use case involving detection of the *EGFR* point mutation T790M in DNA[6]	Exp.	N/A	3904 (not manually curated*)	5720	One-color
D8	Trace Idealization	ACTR-NCBD Binding at 10-ms binning[1,9]	Exp.	N/A	N/A**	19***	Two-color
D9	Biological Discovery	Pre-mRNA conformational changes during yeast splicing[7]	Exp.	N/A	N/A	6805	Two-color
D10	META-SiM Pre-Training	A synthetic dataset of smFRET traces representing diverse dynamics to train META-SiM	Simulated	1.5 million	N/A	N/A	Two-color & One-color
D11	smFRET Atlas Training & Annotation	A synthetic dataset of smFRET traces representing diverse dynamics to train and annotate a global 2D UMAP with META-SiM	Simulated	1.02 million	N/A	N/A	Two-color

* For the dataset D7, the labels for the fine-tuning set was not manually curated, but generated based on the experimental conditions, whereas true for mutant only condition and false for wild-type only condition, same strategy used in our previous work in ref[10].

** D8, D9 use cases didn't involve any fine-tuning. META-SiM foundation model was directly applied in these tasks.

*** The full experiment dataset used in the benchmark study of 14 tools[1], with n(traces) = 19, n(datapoints) = 226,100, using 10 ms time bins resulting in 100 Hz sampling.

Supplementary Table 3. Description and parameter range for generating traces to build the smFRET Atlas, 1 million traces for training and 22,000 traces for annotation. (All ranges in the table represent uniform distributions.)

Code	Description	Number of States	SNR	FRET Values	Kinetic Rate Constant [Frame^{-1}]
1-c-l	1 FRET state, clean, low FRET value	1	[4, 8]	State 1: [0.05, 0.35]	N/A
1-c-m	1 FRET state, clean, middle FRET value	1	[4, 8]	State 1: [0.4, 0.6]	N/A
1-c-h	1 FRET state, clean, high FRET value	1	[4, 8]	State 1: [0.65, 0.95]	N/A
1-n-l	1 FRET state, noisy, low FRET value	1	[1.5, 4]	State 1: [0.05, 0.35]	N/A
1-n-m	1 FRET state, noisy, middle FRET value	1	[1.5, 4]	State 1: [0.4, 0.6]	N/A
1-n-h	1 FRET state, noisy, high FRET value	1	[1.5, 4]	State 1: [0.65, 0.95]	N/A
2-c-lm-s	2 FRET states, clean, middle and low FRET values, slow transition	2	[4, 8]	State 1: [0.05, 0.35] State 2: [0.4, 0.6]	[0.005, 0.025]
2-c-lm-f	2 FRET states, clean, middle and low FRET values, fast transition	2	[4, 8]	State 1: [0.05, 0.35] State 2: [0.4, 0.6]	[0.05, 0.2]
2-c-lh-s	2 FRET states, clean, low and high FRET values, slow transition	2	[4, 8]	State 1: [0.05, 0.35] State 2: [0.65, 0.95]	[0.005, 0.025]
2-c-lh-f	2 FRET states, clean, low and high FRET values, fast transition	2	[4, 8]	State 1: [0.05, 0.35] State 2: [0.65, 0.95]	[0.05, 0.2]
2-c-mh-s	2 FRET states, clean, middle and high FRET values, slow transition	2	[4, 8]	State 1: [0.4, 0.6] State 2: [0.65, 0.95]	[0.005, 0.025]
2-c-mh-f	2 FRET states, clean, middle and high FRET values, fast transition	2	[4, 8]	State 1: [0.4, 0.6] State 2: [0.65, 0.95]	[0.05, 0.2]
2-n-lm-s	2 FRET states, noisy, middle and low FRET values, slow transition	2	[1.5, 4]	State 1: [0.05, 0.35] State 2: [0.4, 0.6]	[0.005, 0.025]
2-n-lm-f	2 FRET states, noisy, middle and low FRET values, fast transition	2	[1.5, 4]	State 1: [0.05, 0.35] State 2: [0.4, 0.6]	[0.05, 0.2]
2-n-lh-s	2 FRET states, noisy, low and high FRET values, slow transition	2	[1.5, 4]	State 1: [0.05, 0.35] State 2: [0.65, 0.95]	[0.005, 0.025]
2-n-lh-f	2 FRET states, noisy, low and high FRET values, fast transition	2	[1.5, 4]	State 1: [0.05, 0.35] State 2: [0.65, 0.95]	[0.05, 0.2]
2-n-mh-s	2 FRET states, noisy, middle and high FRET values, slow transition	2	[1.5, 4]	State 1: [0.4, 0.6] State 2: [0.65, 0.95]	[0.005, 0.025]
2-n-mh-f	2 FRET states, noisy, middle and high FRET values, fast transition	2	[1.5, 4]	State 1: [0.4, 0.6] State 2: [0.65, 0.95]	[0.05, 0.2]

3-c-lmh-s	3 FRET states, clean, low and middle and high FRET values, slow transition	3	[4, 8]	State 1: [0.01, 0.35] State 2: [0.4, 0.6] State 3: [0.65, 0.95]	[0.002, 0.025]
3-c-lmh-f	3 FRET states, clean, low and middle and high FRET values, slow transition	3	[4, 8]	State 1: [0.01, 0.35] State 2: [0.4, 0.6] State 3: [0.65, 0.95]	[0.05, 0.2]
3-n-lmh-s	3 FRET states, noisy, low and middle and high FRET values, slow transition	3	[1.5, 4]	State 1: [0.01, 0.35] State 2: [0.4, 0.6] State 3: [0.65, 0.95]	[0.002, 0.025]
3-n-lmh-f	3 FRET states, noisy, low and middle and high FRET values, slow transition	3	[1.5, 4]	State 1: [0.01, 0.35] State 2: [0.4, 0.6] State 3: [0.65, 0.95]	[0.05, 0.2]

References

1. Götz, M. *et al.* A blind benchmark of analysis tools to infer kinetic rate constants from single-molecule FRET trajectories. *Nat. Commun.* **13**, 5402 (2022).
2. Fu, J. *et al.* Multi-enzyme complexes on DNA scaffolds capable of substrate channelling with an artificial swinging arm. *Nat. Nanotechnol.* **9**, 531–536 (2014).
3. Suddala, K. C., Wang, J., Hou, Q. & Walter, N. G. Mg2+ Shifts Ligand-Mediated Folding of a Riboswitch from Induced-Fit to Conformational Selection. *J. Am. Chem. Soc.* **137**, 14075–14083 (2015).
4. Widom, J. R. *et al.* Ligand Modulates Cross-Coupling between Riboswitch Folding and Transcriptional Pausing. *Mol. Cell* **72**, 541-552.e6 (2018).
5. Suddala, K. C. *et al.* Local-to-global signal transduction at the core of a Mn2+ sensing riboswitch. *Nat. Commun.* **10**, 4304 (2019).
6. Hayward, S. L. *et al.* Ultraspecific and Amplification-Free Quantification of Mutant DNA by Single-Molecule Kinetic Fingerprinting. *J. Am. Chem. Soc.* **140**, 11755–11762 (2018).
7. Blanco, M. R. *et al.* Single Molecule Cluster Analysis Identifies Signature Dynamic Conformations along the Splicing Pathway. *Nat. Methods* **12**, 1077–1084 (2015).
8. Li, J. *et al.* Exploring the speed limit of toehold exchange with a cartwheeling DNA acrobat. *Nat. Nanotechnol.* **13**, 723–729 (2018).
9. Zosel, F., Soranno, A., Buholzer, K. J., Nettels, D. & Schuler, B. Depletion interactions modulate the binding between disordered proteins in crowded environments. *Proc. Natl. Acad. Sci.* **117**, 13480–13489 (2020).
10. Li, J., Zhang, L., Johnson-Buck, A. & Walter, N. G. Automatic classification and segmentation of single-molecule fluorescence time traces with deep learning. *Nat. Commun.* **11**, 5833 (2020).